High-Speed DC Transport of Emergent Monopoles in Spinor Photonic Fluids

H. Terças,* D. D. Solnyshkov, and G. Malpuech
Institut Pascal, PHOTON-N2, Clermont Université, Blaise Pascal University, CNRS, 24 Avenue des Landais, 63177 Aubière Cedex, France

(Received 22 October 2013; revised manuscript received 19 May 2014; published 16 July 2014)

We investigate the spin dynamics of half-solitons in quantum fluids of interacting photons (exciton polaritons). Half-solitons, which behave as emergent monopoles, can be accelerated by the presence of effective magnetic fields. We study the generation of dc magnetic currents in a gas of half-solitons. At low densities, the current is suppressed due to the dipolar oscillations. At moderate densities, a magnetic current is recovered as a consequence of the collisions between the carriers. We show a deviation from Ohm's law due to the competition between dipoles and monopoles.

DOI: 10.1103/PhysRevLett.113.036403 PACS numbers: 71.36.+c, 03.75.Lm, 14.80.Hv

Since the original idea of Dirac [1], magnetic monopoles have been one of the most important physical questions in quantum mechanics. In fact, "real" elementary magnetic charges have not been observed up to now, despite long efforts to detect them [2]. Recently, magnetically frustrated materials, or spin ices [3,4], offered the possibility of investigating magnetic charge transport. Besides the substantial experimental evidence to support the existence of spin-ice magnetic monopoles [5–8], the measurement of the charge and current of magnetic monopoles has become possible [9]. In fact, signatures of emergent magnetic monopoles are present in other systems, such as nanowires [10] and spinor Bose-Einstein condensates [11]. Physically, these monopoles are elementary excitations in the system, or quasiparticles, a concept that is widely used in solid state physics to describe the behavior of carriers in the band structure [12]. Modern electronics, for example, is successfully described in their terms. Quasiparticles differ from "real" particles in the sense that they cannot exist outside the underlying medium.

An interesting example of quasiparticles is the half-solitons (HSs) in spinor Bose-Einstein condensates (BECs). HSs are stable localized excitations of spinor BECs with spin-anisotropic interactions [11,13,14]. Recently, some of us have experimentally demonstrated that they behave like effective magnetic charges, accelerated along effective magnetic fields [11]. HSs are observed in exciton-polariton condensates in microcavities [15] behaving as interacting photon fluids [16]. The monopolar spin texture of HSs results from the spin of photonic particles. Photons do not interact with a real magnetic field [17]. However, as for any two-level system, the coupling between their spin components can be described by Pauli matrices, as an action of an effective magnetic field on a pseudospin. The important difference between artificial electric and magnetic fields is that the latter couples with the spin of particles via the Pauli matrices. The achievement and control of such effective magnetic fields are actively pursued both in atomic BECs [18–20] and photonic systems [21–25]. Electricity, which is the basis of the modern world, is a current of electric charges in applied electric fields. By analogy, the motion of magnetic charges in a magnetic field has been generally referred to as "magnetricity" [9]. Therefore, the idea of using HSs for magnetricity appears both natural and important.

In this work, we present a theoretical study of monopole transport with HS gases: the collective motion of emergent monopoles in the presence of an effective magnetic field. We show that at very low gas densities, the conductivity is suppressed due to dipole oscillations. At higher densities, when collisions between HSs are more likely, the magnetic conductivity is optimal. For very dense gases, the conductivity decreases as a consequence of the collision time shortening. We also predict a deviation from the magnetic Ohm's law $j \propto H$ for moderate magnitudes of the applied field H. To confirm our predictions based on a kinetic model, we perform numerical simulations of realistic experimental configurations, where the dc conductivity can be effectively measured. Finally, we estimate the mobility of magnetic charges to 10^7 cm^2/V s. This value is an order of magnitude larger than the record value of the electronic mobility in graphene [26,27] and confirms the anticipated advantage of using photonic magnetic monopoles [28] over other systems for application purposes.

Relativistic dynamics of half-solitons.—Exciton polaritons are bosonic quasiparticles that result from strong light-matter coupling in semiconductor microcavities. Their most important properties in the framework of the present study are their capacity to form a condensate, their small effective mass, and a very strong nonlinearity. Exciton-polariton condensates in one-dimensional systems can be described by the spinor Gross-Pitaevskii equation [16,29]

$$i\hbar\frac{\partial\psi_\pm}{\partial t} = -\frac{\hbar^2}{2m}\Delta\psi_\pm + \alpha_1|\psi_\pm|^2\psi_\pm + \alpha_2|\psi_\mp|^2\psi_\pm - H\psi_\mp, \quad (1)$$

where $\boldsymbol{\psi} = (\psi_+, \psi_-)$ is the spinor representing two circular polarizations [29]. Here, $\mathbf{H} = H\mathbf{e}_x$ is the effective magnetic field, describing the longitudinal-transverse splitting due to the confinement [30]. Exciton polaritons are also characterized by a strong spin anisotropy (typically, $-0.2\alpha_1 \lesssim \alpha_2 \lesssim -0.1\alpha_1$), which allows the existence of half-integer topological defects, such as half-solitons and half-vortices [31], which can be written as a scalar soliton in a single spin component $\psi(x) = \sqrt{n_0}\tanh(x/\sqrt{2}\xi)$, with the healing length $\xi = \hbar/\sqrt{2\alpha_1 m n_0}$ [32–34]

$$\psi_+ = \sqrt{\frac{n_0}{2}}\left[i\frac{v}{c} + \frac{1}{\gamma}\tanh\left(\frac{x-y}{\sqrt{2}\xi\gamma}\right)\right], \qquad \psi_- = \sqrt{\frac{n_0}{2}}. \quad (2)$$

Here, the half-soliton propagates with a velocity v, $y = vt + x_0$ is the soliton centroid, $c = \sqrt{\alpha_1 n_0/m}$ is the sound speed, and $\gamma = (1 - v^2/c^2)^{-1/2}$ is the relativistic factor. This solution is characterized by a divergent in-plane pseudospin pattern $S_x = \mathrm{Re}(\psi_+\psi_-^*)/2 \simeq (n_0/2\gamma)\mathrm{sgn}(y-x)$. Figure 1(a) shows the density and the pseudospin for two HSs in opposite spin components. The magnetic charge is defined by analogy with Maxwell's equation $\rho = \nabla\cdot\mathbf{S}$, and the charge of a single HS is $q = \pm n/2 = \pm n_0/2\gamma$ (as shown by the plus and minus symbols in Fig. 1). Since the charge is defined by the in-plane pseudospin texture, it does not depend on the $\sigma_\pm$ component in which the HS appears. The dynamics of each spin in a magnetic field is governed by the precession equation $\partial\mathbf{S}/\partial t = \mathbf{S}\times\mathbf{H}$. The monopole

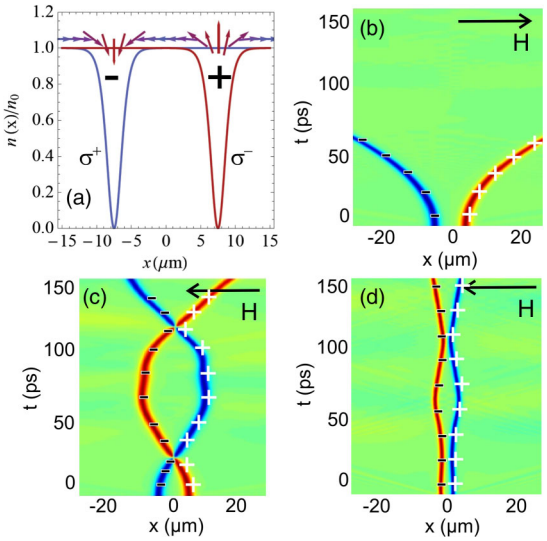

FIG. 1 (color online). Polarization degree ρ_c for a pair of half-solitons. (a) The red (dark gray) [blue (light gray)] line depicts the density profile of a half-soliton in the $\sigma = -$ [$\sigma = +$] component. The arrows indicate the pseudospin S_x. Numerical time evolution of ρ_c as extracted from Eq. (1) in the presence of a constant magnetic field $\mathbf{H} = \pm 10\mathbf{e_x}\ \mu$eV (black arrows), showing the trajectories of two HSs: (b) acceleration for $H > 0$, (c) oscillations, and (d) bouncing for $H < 0$. The plus and minus symbols indicate the sign of the magnetic charges.

dynamics of Eq. (2) can be obtained by calculating the magnetic force $F_m = -n_0 H/2\gamma$ and the acceleration $a = n_0 H/2M_0\gamma^2$, where $M_0 = 2\sqrt{2}n_0\xi m$ is the absolute value of the HS rest mass [35]. Integrating once, the velocity is $v(t) = c\tanh(t/\tau_0)$ [36], where $\tau_0 = 2M_0 c/n_0 H$, which means that the soliton cannot be accelerated above the sound speed c. This trajectory is reproduced by numerical simulations of Eq. (1).

Spin dynamics.—Let us now consider *two* HS solutions for the spinor condensate $[\boldsymbol{\psi} = (\psi_+, \psi_-)]$, resulting from the superposition of solitons in each of the spin components, located at the positions $\pm y/2$

$$\psi_\pm = \sqrt{\frac{n_0}{2}}\left[\pm i\frac{\dot{y}}{c} + \frac{1}{\gamma}\tanh\left(\frac{x \mp y/2}{\sqrt{2}\xi\gamma}\right)\right]. \quad (3)$$

Notice that this solution is different from the kink-antikink solution [37], which consists of a product of solitons within the same spin component. Equation (3) will be used to model the soliton gas in the second part of the paper. The pseudospin texture is invariant with respect to the exchange of the two HSs $y \to -y$: for this particular solution, the spin field is divergent for the soliton on the right. Moreover, to assure the continuity of the phase, it is impossible to have two solitons of the same type (kink-kink) next to each other. Figure 1, therefore, is the most general spin texture. When two solitons cross each other, the "sign" of each monopole is inverted; i.e., the one located in the σ_- projection, initially with a convergent texture, becomes divergent after crossing, and vice versa. In Figs. 1(b)–1(d), we depict the temporal evolution of the polarization degree $\rho_c = (n_+ - n_-)/(n_+ + n_-)$ of the HS by solving Eq. (1). Figure 1(b) illustrates the simplest behavior: acceleration without crossing for $H > 0$; Fig. 1(c) illustrates the inversion of the charge (the "red" σ_- soliton is initially accelerated to the left and then to the right). In this case, the two solitons undergo dipolar oscillations, forming a "molecule," due to the inversion of the spin texture (charge). Figure 1(d) depicts the bouncing of the two HSs without the charge inversion, due to the interactions between spin components. We note the repulsive interaction between solitons for $\alpha_2 < 0$, as a consequence of their negative mass [38].

We proceed to a variational analysis of the spin dynamics by using Eq. (3) as an ansatz. The variational energy $E[y, \dot{y}] = \int \mathcal{E}dx$, with $\mathcal{E} = \sum_{\sigma=\pm}[(\hbar^2/2m)|\psi_\sigma|^2 + (1/2)\alpha_1(|\psi_\sigma|^2 - (n_0/2))^2] + \alpha_2(|\psi_+|^2|\psi_-|^2 - (n/2)) - \mathrm{HS}_x$ representing the energy density [32,33], is given by

$$E[y,\dot{y}] = \frac{4\sqrt{2}}{3}\left(1 - \frac{\dot{y}^2}{c^2}\right)^{3/2}\alpha_1 n_0^2\xi + \sqrt{2}Hn_0\xi\zeta\coth(\zeta) + \sqrt{2}\left(1 - \frac{\dot{y}^2}{c^2}\right)^{3/2}\alpha_2 n_0^2\xi\frac{\sinh(\zeta) - \zeta\cosh(\zeta)}{\sinh^3(\zeta)}, \quad (4)$$

where $\zeta = y(1 - \dot{y}^2/c^2)^{1/2}/\sqrt{2}\xi$. The dynamics of a HS pair can then be calculated via the Hamilton equations

$\partial E/\partial y + d/dt(\partial E/\partial \dot{y}) = 0$ and corresponds to that of a relativistic anharmonic oscillator. We restrict our discussion to the case of attractive interspin interaction $\alpha_2 = -0.2\alpha_1$. The results are summarized in Fig. 2(a). If the solitons are accelerated away from each other ($H > 0$), their trajectories correspond to open orbits in the phase space; on the contrary, if accelerated towards each other, nonlinear oscillations of the HS molecule take place. Because of the competition between the short-range repulsion and the magnetic force, the system exhibits three types of oscillations, depending on the initial separation $d \equiv y(t = 0)$: below the critical field H_1, defined through the condition $\partial E/\partial y|_{\dot{y}=0} = 0$, repulsion dominates and the solitons bounce at distances larger than d [mode I, also shown in Fig. 1(d)]; for $H_1 < H < H_2$, with H_2 defined by the contour $E|_{\dot{y}=0} = 0$, dipolar oscillations possess an amplitude smaller than the initial separation d (mode II); finally, for $H > H_2$, the solitons oscillate by crossing each other [mode III, also in Fig. 1(c)]. The critical fields H_1 and H_2 for the different oscillatory modes are shown in Fig. 2(b). For small-amplitude oscillations $d \lesssim \xi$, the dynamics is given by the equation $\ddot{y} + \omega^2 y = 0$ and the oscillation frequency is

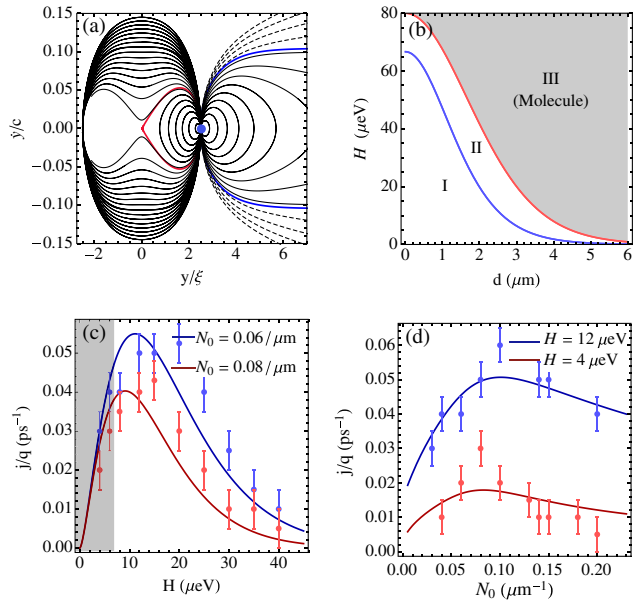

FIG. 2 (color online). (a) Phase-space map for a pair of half-solitons initially separated by $d = 2.5\xi$. Solid (dashed) lines are obtained for $H > 0$ ($H < 0$). The thick line is obtained for $H = 0$. The red (dark gray) line is the separatrix between modes II and III. (b) Magnitude of the critical fields H_1 [red (dark gray) line] and H_2 [blue (light gray) line] as a function of the initial separation d. The dc monopole current as a function of the applied field [gas density] is shown in (c) [(d)]. The shadow limits the Ohmic region. (c),(d) Solid lines are the theoretical predictions and the dots with error bars are the numerical results. Other parameters: $m = 5 \times 10^{-5} m_e$, $\xi = 1$ μm, and $n_0 \sim 500$ μm^{-1}.

$$\omega = \frac{c_s}{\xi}\left(\frac{5H - 4\alpha_2 n_0}{15(H + 4\alpha_1 n_0 + 2\alpha_2 n_0)}\right)^{1/2}. \quad (5)$$

A set of half-solitons: The soliton gas.—We consider a dense soliton gas, for which the multiple soliton solution with the inverse scattering transform [39] provides a continuum of eigenvalues. In that case, the solitons are uncorrelated and therefore ergodic enough to justify a statistical treatment. Kinetic equations have been used to describe wave turbulence in optical fibers [40]. A detailed kinetic model of an uncorrelated dense soliton gas has been provided in Ref. [41], and its collective behavior has been addressed in Refs. [37,42] and by us in Ref. [38]. Motivated by these results, we describe the evolution of the distributions $f^{\pm}(x, v, t)$ with the following kinetic equations of the Boltzmann type:

$$\frac{\partial f^{\pm}}{\partial t} + v\frac{\partial f^{\pm}}{\partial x} + \frac{q(v)}{M(v)}H\frac{\partial f^{\pm}}{\partial v} = I[f^{\pm}], \quad (6)$$

where $q(v)/M(v) = n_0/2M_0\gamma^2$ is the relativistic charge-mass ratio. Interesting features like dynamic crystallization have also been captured with kinetic equations of this type [38,43,44]. In order to estimate the transport properties of the system, in analogy with the Drude model for electrons in the presence of an electric field [45], we assume small departures from equilibrium, allowing for the collision integral $I[f^{\pm}]$ to be written in the relaxation-time approximation [46] $I[f^{\pm}] \simeq -(f^{\pm} - f_0^{\pm})/\tau^{\pm}$, where $\tau^{\pm}$ is the relaxation time and $f_0^{\pm}$ is the phase-space equilibrium distribution. We define the total magnetic current as $j = j^{+} - j^{-}$, where $j^{\sigma} = \langle q(v)N_c v\rangle = \int q(v)N_c v f^{\sigma} dv$ and N_c is the concentration of magnetic charges. For symmetry, the total current is given as $j = 2j^{+} = -2j^{-}$, so we calculate the current associated with the σ_{+} component, thus dropping the superscript in the equations above. From Eq. (6), the dc magnetic current can be written as

$$j = \frac{N_c n_0^2 \tau}{2M_0} H \int v\left(1 - \frac{v^2}{c^2}\right)\frac{\partial f_0}{\partial v} dv. \quad (7)$$

Equation (7) incorporates the relativistic behavior of HSs, which implies a vanishing current near the sound speed $v \simeq c$. To estimate the collision time τ, we make use of the Matthiessen's rule [47]: $1/\tau = 1/\tau_H + 1/\tau_{\sigma,\sigma} + 1/\tau_{\sigma,-\sigma}$, where τ_H is the collision rate induced by the field H; $\tau_{\sigma,\sigma}$ (respectively, $\tau_{\sigma,-\sigma}$) represents the collision rate due to the short-range (but not contact) topological interaction between solitons of the same (respectively, opposed) spin projection [33,38]. A detailed derivation of τ is provided in the Supplemental Material [48].

The two-body dynamics is in competition with the collective behavior of the system. Thus, the concentration of available monopoles is not necessarily the same as that of the gas. To estimate the concentration of carriers, we

extend Onsager's theory for the conduction of weak electrolytes [48,49]. Using the fermionic statistics of solitons $f_0 = N_0/(2v_F)\Theta(v_F - v)$ [38], Eq. (7) yields

$$j = \frac{N_0 n_0^2}{2M_0}\tau H\eta\left(1 - \frac{v_F^2}{c^2}\right), \tag{8}$$

with η standing for the fraction of dissociated monopoles. The Fermi velocity of the gas $v_F = \pi\hbar N_0/M_0$ is small compared to the sound speed for the case of polariton condensates, but it is not necessarily the case for cold atomic condensates—indeed, the same calculations could be performed for the latter—for which we may have $n_0\xi \sim 1$. The features of Eq. (8) are summarized in Figs. 2(c) and 2(d). For small values of the field, η does not vary with H and the dc current satisfies the Ohm's law $j \propto H$ [see Fig. 2(c)]. For moderate values of H, the system enters a non-Ohmic regime, characterized by $\partial j/\partial H < 0$. This behavior is qualitatively different from the deviation from the Ohmic response observed in spin ices, where the conductivity monotonically increases with the applied field [9]. The reason for such a difference resides in the fact that the soliton-pair dissociation energy depends on the density of the HS gas; besides, our system is 1D and the jamming of carriers is more important than in spin ices. In Fig. 2(d), we plot the conductivity against the HS gas density. For very low densities, the transport is dominated by two-particle dynamics and the dc current is strongly suppressed. For higher densities, the response of the system is dictated by collisions. As a consequence, the magnetic conductivity reaches its maximum for moderate densities ($N_0 \approx 0.12\ \mu\text{m}^{-1}$ for $H = 6\ \mu$eV).

We have also performed numerical simulations using Eq. (1) with a gas of HS taken as an initial condition. In Fig. 3, we illustrate the most relevant regimes of the magnetic current. In Fig. 3(a), we observe the breaking of dipolar oscillations (or molecule dissociation) due to collisions between the solitons within the same component. For moderate values of density [Fig. 3(b)], such collisions, similarly to the Drude model for electron conduction, lead to the appearance of a net current of magnetic charges (Ohmic response). Finally, for higher values of density, the conductivity is suppressed [Fig. 3(c)], and the small-amplitude oscillations become the dominant mechanism. All these features are in qualitative agreement with the analytical estimates, as illustrated in Fig. 2. The deviation between the analytic theory and the numerical results may stem in the fact that the transport model neglects the acoustic radiation of solitons as they accelerate [50]. We moreover notice that quantum fluctuations are neglected, as solitons are here treated as classical particles. Therefore, a more suitable treatment of the transport properties might be done in the framework of Luttinger theory [38,51,52], which would eventually capture additional features beyond the present mean-field approach.

To describe a more realistic experimental configuration (see Ref. [48] for details), we simulate Eq. (1) for polaritons

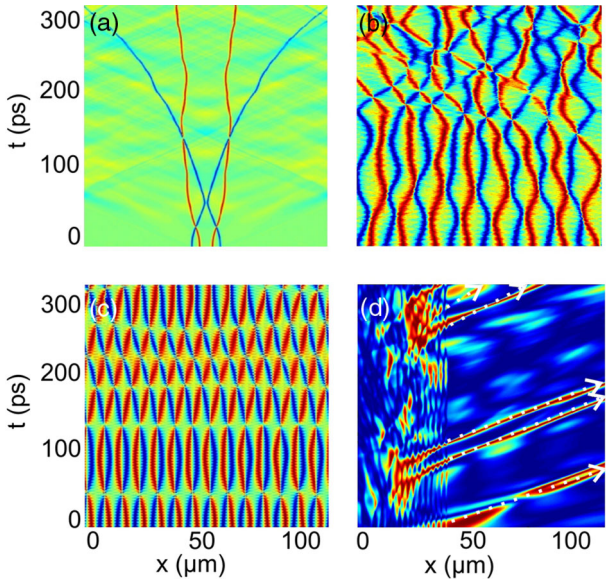

FIG. 3 (color online). (a) Breakdown of oscillations due to the interactions between HSs in the same component. (b) The onset of magnetricity ($N_0 \sim 0.08\ \mu\text{m}^{-1}$). (c) Suppression of conductivity due to short-range interaction ($N_0 \sim 0.15\ \mu\text{m}^{-1}$). (d) Extraction of half-solitons (red traces) from the trapping region ($\lambda = 0.5\ \mu$m, $L = 45\ \mu$m, $U_0 = 2$ meV, and $\tau = 30$ ps) by a field $H = 5\ \mu$eV. The white arrows are a guide for the eyes.

propagating in a one-dimensional cavity by adding (i) a narrow Gaussian barrier described by the potential $U_\pm\psi_\pm = U_0\exp[-(x-L)^2/\lambda^2]\psi_\pm$, (ii) a coherent, linearly polarized pump $P_\pm = P_0(x)e^{i(kx-\omega t)}$, and (iii) the finite lifetime term $-i\hbar\psi_\pm/2\tau$. The barrier, located at the position $x = L$, is strong enough to confine the HS gas. Initially, the magnetic field is absent, and the solitons remain trapped without escaping. Then, the effective magnetic field is switched on (it can be controlled externally [53]), and we observe the extraction of HS from the confined region [red traces propagating to the right in Fig. 3(d)], showing the linear polarization degree of the condensate. An alternative way of generating soliton trains has recently been proposed [54].

The monopole mobility can be directly estimated from our calculations, for which we compare the potential energies corresponding to a fixed displacement. Indeed, a mobility of $10^6\ \text{cm}^2/\text{V s}$ (a record value obtained in graphene [26,27]) means that an electron is accelerated up to a speed a of 10^6 cm/s in a field of 1 V/cm. The same displacement of a half-soliton corresponds to a magnetic energy of 10 eV (assuming $n_0 \sim 2\times 10^2\ \mu\text{m}^{-1}$ and a Zeeman splitting of 5 μeV), while the velocity is $\sim 10^8$ cm/s, which provides an equivalent mobility of $\mu = 10^7\ \text{cm}^2/\text{V s}$. Such a high value is due to the extremely low polariton mass ($m < 10^{-4}m_e$).

To conclude, we have studied the transport properties of a gas of half-solitons in spinor polariton condensates in the presence of an effective dc magnetic field. We found that the monopole current deviates from the Ohmic response

due to the competition of half-soliton oscillations and collisions. Record values of mobility can be expected due to the low polariton mass.

The authors acknowledge the support of the EU POLAPHEN, ANR Quandyde, and GANEX projects.

*htercas@gmail.com

[1] P. Dirac, Proc. R. Soc. A **133**, 60 (1931).
[2] J. L. Pinfold, AIP Conf. Proc. **1304**, 234 (2010).
[3] M. J. Harris, S. T. Bramwell, D. F. McMorrow, T. Zeiske, and K. W. Godfrey, Phys. Rev. Lett. **79**, 2554 (1997).
[4] C. Castelnovo, R. Moessner, and S. L. Sondhi, Nature (London) **451**, 42 (2007).
[5] L. D. C. Jaubert and P. C. W. Holdsworth, Nat. Phys. **5**, 258 (2009).
[6] T. Fennel, P. P. Deen, A. R. Wildes, K. Schmalzl, D. Prabhakaran, A. T. Boothroyd, R. J. Aldus, D. F. McMorrow, and S. T. Bramwell, Science **326**, 415 (2009).
[7] D. J. P. Morris *et al.*, Science **326**, 411 (2009).
[8] H. Kadowaki, N. Doi, Y. Aoki, Y. Tabata, T. J. Sato, J. W. Lynn, K. Matsuhira, and Z. Hiroi, J. Phys. Soc. Jpn. **78**, 103706 (2009).
[9] S. T. Bramwell, S. R. Gibli, S. Calde, R. Aldu, D. Prabhakaran, and T. Fennell, Nature (London) **461**, 956 (2009).
[10] S. S. P. Parkin, M. Hayashi, and L. Thomas, Science **320**, 190 (2008).
[11] R. Hivet *et al.*, Nat. Phys. **8**, 724 (2012).
[12] L. D. Landau, Sov. Phys. JETP **3**, 920 (1956); **5**, 101 (1957).
[13] H. Flayac, D. D. Solnyshkov, and G. Malpuech, Phys. Rev. B **83**, 193305 (2011); New J. Phys. **14**, 085018 (2012).
[14] H. Flayac, D. D. Solnyshkov, I. A. Shelykh, and G. Malpuech, Phys. Rev. Lett. **110**, 016404 (2013).
[15] A. Kavokin, J. J. Baumberg, F. P. Laussy, and G. Malpuech, *Microcavities* (Oxford University Press, New York, 2008).
[16] I. Carusotto and C. Ciuti, Rev. Mod. Phys. **85**, 299 (2013).
[17] Contrary to pure photonic states, exciton polaritons do interact with a real magnetic field via the charges constituting their excitonic part.
[18] Y.-J. Lin, R. L. Compton, K. Jiménez-García, J. V. Porto, and I. B. Spielman, Nature (London) **462**, 628 (2009).
[19] Y.-J. Lin, K. Jiménez-García, and I. B. Spielman, Nature (London) **471**, 83 (2011).
[20] J. Dalibard, F. Gerbier, G. Juzeliünas, and P. Öhberg, Rev. Mod. Phys. **83**, 1523 (2011).
[21] R. O. Umucalilar and I. Carusotto, Phys. Rev. A **84**, 043804 (2011).
[22] M. Hafezi, E. A. Demler, M. P. Lukin, and J. M. Taylor, Nat. Phys. **7**, 907 (2011).
[23] M. Hafezi, J. Fan, A. Migdall, and J. Taylor, Nat. Photonics **7**, 1001 (2013).
[24] M. C. Rechtsman, J. M. Zeuner, A. Tnnermann, S. Nolte, M. Segev, and A. Szameit, Nat. Photonics **7**, 153 (2013).
[25] M. C. Rechtsman, J. M. Zeuner, Y. Plotnik, Y. Lumer, D. Podolsky, F. Dreisow, S. Nolte, M. Segev, and A. Szameit, Nature (London) **496**, 196 (2013).
[26] K. S. Novoselov, "Nobel Lecture," 2010 (unpublished).
[27] K. I. Bolotin, K. J. Sikes, Z. Jiang, M. Klima, G. Fudenberg, J. Hone, P. Kim, and H. L. Stormer, Solid State Commun. **146**, 351 (2008).
[28] S. T. Bramwell, Nat. Phys. **8**, 703 (2012).
[29] I. A. Shelykh, Y. G. Rubo, G. Malpuech, D. D. Solnyshkov, and A. Kavokin, Phys. Rev. Lett. **97**, 066402 (2006).
[30] L. Klopotowski, M. D. Martin, A. Amo, L. Vina, I. A. Shelykh, M. M. Glazov, G. Malpuech, A. V. Kavokin, and R. Andre, Solid State Commun. **139**, 511 (2006).
[31] K. G. Lagoudakis, T. Ostatnicky, A. V. Kavokin, Y. G. Rubo, R. Andre, and B. Deveaud-Pledran, Science **326**, 974 (2009).
[32] L. Pitaevskii and S. Stringari, *Bose-Einstein Condensation* (Oxford Science, New York, 2003).
[33] P. Öhberg and L. Santos, Phys. Rev. Lett. **86**, 2918 (2001).
[34] D. J. Frantzeskakis, J. Phys. A **43**, 213001 (2010).
[35] The mass of each soliton is defined by the number of polaritons depleted from the condensate $M = m\int \psi_{\pm}^{*}\psi_{\pm} dx = -2\sqrt{2}n_0\xi m/\gamma$, therefore being negative. M_0 is here defined as the magnitude of the rest mass.
[36] D. D. Solnyshkov, H. Flayac, and G. Malpuech, Phys. Rev. B **85**, 073105 (2012).
[37] B. A. Malomed, A. Schwache, and F. Mitschke, Fiber Integr. Opt. **17**, 267 (1998); B. A. Malomed and A. A. Nepomnyashchy, Europhys. Lett. **27**, 649 (1994); P. Franco, F. Fontana, L. Cristiani, M. Midrio, and M. Romagnoli, Opt. Lett. **20**, 2009 (1995).
[38] H. Terças, D. D. Solnyshkov, and G. Malpuech, Phys. Rev. Lett. **110**, 035303 (2013).
[39] V. E. Zakharov, JETP Lett. **33**, 538 (1971).
[40] V. E. Zakharov, Stud. Appl. Math. **122**, 219 (2009); D. B. S. Soh, J. P. Koplow, S. W. Moore, K. L. Schroder, and W. L. Hsu, Opt. Express **18**, 22393 (2010); P. Suret, A. Picozzi, and S. Randoux, Opt. Express **19**, 17852 (2011).
[41] G. A. El and A. M. Kamchatnov, Phys. Rev. Lett. **95**, 204101 (2005).
[42] A. Fratalocchi, C. Conti, G. Ruocco, and S. Trillo, Phys. Rev. Lett. **101**, 044101 (2008).
[43] A. Haboucha, H. Leblond, M. Salhi, A. Komarov, and F. Sanchez, Opt. Lett. **33**, 524 (2008).
[44] S. Rutz and F. Mitschke, J. Opt. B **2**, 364 (2000).
[45] P. Drude, Ann. Phys. (Berlin) **306**, 566 (1900); A. Sommerfeld, Z. Phys. **47**, 1 (1928).
[46] V. F. Gantmakher and Y. B. Levinson, *Carrier Scattering in Metal and Semiconductors* (North-Holland, Amsterdam, 1987).
[47] T. P. Beaulac, P. B. Allen, and F. J. Pinski, Phys. Rev. B **26**, 1549 (1982).
[48] See the Supplemental Material at http://link.aps.org/supplemental/10.1103/PhysRevLett.113.036403 for details on the calculation of the monopole conductivity in Eq. (7).
[49] L. Onsager, J. Chem. Phys. **2**, 599 (1934).
[50] N. G. Parker, N. P. Proukakis, C. F. Barenghi, and C. S. Adams, J. Phys. B **37**, S175 (2004).
[51] I. Safi, Eur. Phys. J. B **12**, 451 (1999).
[52] I. Safi and H. Saleur, Phys. Rev. Lett. **93**, 126602 (2004).
[53] G. Malpuech, M. M. Glazov, I. A. Shelykh, P. Bigenwald, and K. V. Kavokin, Appl. Phys. Lett. **88**, 111118 (2006).
[54] F. Pinsker and H. Flayac, Phys. Rev. Lett. **112**, 140405 (2014).